Physics Letters B 709 (2012) 229–233

Contents lists available at SciVerse ScienceDirect

Physics Letters B

www.elsevier.com/locate/physletb

Generalization of radiative jet energy loss to non-zero magnetic mass

Magdalena Djordjevic [a,*], Marko Djordjevic [b]

[a] Institute of Physics Belgrade, University of Belgrade, Serbia
[b] Faculty of Biology, University of Belgrade, Serbia

ARTICLE INFO

Article history:
Received 22 August 2011
Received in revised form 7 February 2012
Accepted 8 February 2012
Available online 9 February 2012
Editor: W. Haxton

ABSTRACT

Reliable predictions for jet quenching in ultra-relativistic heavy ion collisions require accurate computation of radiative energy loss. While all available energy loss formalisms assume zero magnetic mass – in accordance with the one-loop perturbative calculations – different non-perturbative approaches report a non-zero magnetic mass at RHIC and LHC. We here generalize a recently developed energy loss formalism in a realistic finite size QCD medium, to consistently include a possibility for existence of non-zero magnetic screening. We also present how the inclusion of finite magnetic mass changes the energy loss results. Our analysis suggests a fundamental constraint on magnetic to electric mass ratio.

1. Introduction

Jet suppression is considered to be a powerful tool to study the properties of a QCD medium created in ultra-relativistic heavy ion collisions [1–3]. The suppression results from the energy loss of high energy partons moving through the plasma [4]. Therefore, reliable computations of jet energy loss are essential for the reliable predictions of jet suppression. Consequently, a number of different approaches for calculating jet energy loss were developed [5,6, 9–16]. In particular, in [5,6], a theoretical formalism for the calculation of the first order in opacity radiative energy loss in a dynamical QCD medium was developed (see also a viewpoint in [17]). That study models radiative energy loss for all types of quarks in a realistic *finite size* QCD medium with *dynamical* constituents, therefore removing a major approximation of static scattering centers present in previous calculations (see e.g. [9–15]).

While different non-perturbative approaches [18–21] suggest a non-zero magnetic mass at RHIC and LHC, all energy loss calculations up to now [5,6,9–16] assume the absence of magnetic screening. In particular, the dynamical energy loss formalism [5,6] is based on HTL perturbative QCD, which requires zero magnetic mass. The goal of this Letter is to bridge the difference between non-perturbative approaches and energy loss calculations with respect to magnetic screening, and to consistently include magnetic mass in the dynamical energy loss formalism.

We will here consider magnetic mass corrections to the first order in opacity energy loss. Since recent studies [7,8] suggest that higher order corrections to the energy loss are also relevant, an important extension of the work presented here would include generalizing the magnetic mass corrections to higher orders in opacity energy loss calculations.

2. Theoretical analysis

In [5,6], we used finite temperature field theory (HTL approximation) and calculated the radiative energy loss in a finite size dynamical QCD medium. The obtained expression for the energy loss is given by

$$\frac{\Delta E_{\mathrm{rad}}}{E} = \frac{C_R \alpha_s}{\pi} \frac{L}{\lambda_{\mathrm{dyn}}} \int dx \frac{d^2k}{\pi} \frac{d^2q}{\pi} v(\boldsymbol{q}) f(\boldsymbol{k},\boldsymbol{q},x), \tag{2.1}$$

where

$$f(\boldsymbol{k},\boldsymbol{q},x) = 2\left(1-\frac{\sin\frac{(\boldsymbol{k}+\boldsymbol{q})^2+\chi}{xE^+}L}{\frac{(\boldsymbol{k}+\boldsymbol{q})^2+\chi}{xE^+}L}\right)\frac{(\boldsymbol{k}+\boldsymbol{q})}{(\boldsymbol{k}+\boldsymbol{q})^2+\chi} \times\left(\frac{(\boldsymbol{k}+\boldsymbol{q})}{(\boldsymbol{k}+\boldsymbol{q})^2+\chi}-\frac{\boldsymbol{k}}{\boldsymbol{k}^2+\chi}\right). \tag{2.2}$$

In Eqs. (2.1) and (2.2), L is the length of the finite size dynamical QCD medium and E is the jet energy. $\boldsymbol{k}$ is transverse momentum of radiated gluon, while $\boldsymbol{q}$ is transverse momentum of the exchanged (virtual) gluon. $\alpha_s = \frac{g^2}{4\pi}$ is coupling constant and $C_R = \frac{4}{3}$. $v(\boldsymbol{q})$ is the effective cross section in dynamical QCD medium and $\lambda_{\mathrm{dyn}}^{-1} \equiv C_2(G)\alpha_s T = 3\alpha_s T$ $(C_2(G) = 3)$ is called "dynamical mean free path" (see [22,23]). $\chi \equiv M^2x^2 + m_g^2$, where x is the longitudinal momentum fraction of the heavy quark carried away by the emitted gluon, M is the mass of the heavy quark, $m_g = \mu_E/\sqrt{2}$ is the effective mass for gluons with hard momenta $k > T$ [24],

* Corresponding author.
E-mail address: magda@ipb.ac.rs (M. Djordjevic).

0370-2693/$ – see front matter
doi:10.1016/j.physletb.2012.02.019

and μ_E is the Debye mass. We assume constant coupling g. Furthermore, we note that in Eq. (2.1) effective cross section $v(\boldsymbol{q})$ represents the interaction between the jet and exchanged gluon, while $f(\boldsymbol{k},\boldsymbol{q},x)$ represents the interaction between the jet and radiated gluon [5,6].

The goal of this section is to start from the above expression, and generalize it to include the existence of non-zero magnetic mass [18–21]. We first note that the constant $\frac{C_R\alpha_s}{\pi}\frac{L}{\lambda_{\mathrm{dyn}}} = 3\frac{C_R\alpha_s^2}{\pi}TL$ in Eq. (2.1) does not change with the introduction of magnetic mass: note that the coupling constant α_s comes from vertices involving highly energetic jets, while temperature T comes from the Bose–Einstein factor in the soft approximation [23,25]. Therefore, only the integrand in Eq. (2.1) can be modified with the introduction of magnetic mass.

To proceed, we note that the inclusion of magnetic mass modifies the gluon self energy, and therefore our goal is to study how modified self energy of radiated and exchanged gluons change the energy loss result. Furthermore, from [5], it is straightforward to show that non-zero magnetic mass does not alter the factorization ($v(\boldsymbol{q})f(\boldsymbol{k},\boldsymbol{q},x)$) in the integrand of Eq. (2.1), due to the fact that the factorization does not depend on specific form of self energy. Since $v(\boldsymbol{q})$ depends only on the exchanged gluon self energy, while $f(\boldsymbol{k},\boldsymbol{q},x)$ depends only on a radiative gluon self energy, we below separately study how the inclusion of magnetic mass will modify $v(\boldsymbol{q})$ and $f(\boldsymbol{k},\boldsymbol{q},x)$.

2.1. Modification of the effective cross section due to magnetic screening

The effective cross section $v(\boldsymbol{q})$ can be written in the following form

$$v(\boldsymbol{q}) = v_L(\boldsymbol{q}) - v_T(\boldsymbol{q}), \tag{2.3}$$

where $v_T(\boldsymbol{q})$ ($v_L(\boldsymbol{q})$) is transverse (longitudinal) contribution to the effective cross section, given by [5,25,26]

$$v_{T,L}(\boldsymbol{q}) = \frac{1}{\boldsymbol{q}^2 + \mathrm{Re}\,\Pi_{T,L}(\infty)} - \frac{1}{\boldsymbol{q}^2 + \mathrm{Re}\,\Pi_{T,L}(0)}, \tag{2.4}$$

where Π_T and Π_L are gluon self energies. While in [5,6] the derivation of the effective cross section was made through a hard thermal loop for the self-energy Π, one should note that the cross section does not depend on specific form of gluon self energy [25]. That is, the expression is valid for any self-energy satisfying the following assumptions [25]:

1. Π depends only on $x \equiv k_0/k$,
2. $\mathrm{Im}\,\Pi(x=0) = 0$,
3. $\mathrm{Im}\,\Pi(x) = 0$ if $x \geqslant 1$,
4. $\mathrm{Re}\,\Pi(x) \geqslant 0$ if $x \geqslant 1$,

which are reasonable approximations for any system of well defined quasiparticles.

Therefore, we see that the result given by Eq. (2.4) depends only on four numbers: $\mathrm{Re}\,\Pi_{T,L}(\infty)$ and $\mathrm{Re}\,\Pi_{T,L}(0)$; due to this, we don't need to know the full gluon propagator to generalize the effective cross section to the case of finite magnetic screening. The first two numbers are the masses of the longitudinal and the transverse gluons at zero momentum (so-called plasmon masses). These are shown to be equal due to Slavnor–Taylor identities [27–29], which physically means that there is no way to distinguish transverse and longitudinal modes for a particle at rest [25]. Therefore, we need only to introduce one plasmon mass:

$$\mathrm{Re}\,\Pi_T(\infty) = \mathrm{Re}\,\Pi_L(\infty) \equiv \mu_{pl}^2. \tag{2.5}$$

The second two quantities ($\mathrm{Re}\,\Pi_{T,L}(0)$) are squares of the screening masses for the transverse and longitudinal static gluon exchanges. The longitudinal (electric) screening mass is the familiar Debye mass:

$$\mu_E^2 \equiv \mathrm{Re}\,\Pi_L(0). \tag{2.6}$$

In the HTL approximation, there is no screening for the transverse static gluons, but this is not expected to hold generally. The corresponding screening mass is the magnetic mass, and is denoted

$$\mu_M^2 \equiv \mathrm{Re}\,\Pi_T(0). \tag{2.7}$$

The general expressions for the transverse and longitudinal contributions to the effective cross sections $v_{T,L}(\boldsymbol{q})$ then become

$$v_{L,T}(\boldsymbol{q}) = \frac{1}{(\boldsymbol{q}^2 + \mu_{pl}^2)} - \frac{1}{(\boldsymbol{q}^2 + \mu_{E,M}^2)}. \tag{2.8}$$

After replacing the expressions for $v_{L,T}(\boldsymbol{q})$ from Eq. (2.8) into Eq. (2.3), we finally obtain the expression for the effective cross section in the case of non-zero magnetic mass:

$$v(\boldsymbol{q}) = \frac{\mu_E^2 - \mu_M^2}{(\boldsymbol{q}^2 + \mu_M^2)(\boldsymbol{q}^2 + \mu_E^2)}. \tag{2.9}$$

Note that dependence on the plasmon mass drops out of $v(\boldsymbol{q})$ (Eq. (2.9)). This seems reasonable given that $v(\boldsymbol{q})$ involves only space-like gluon exchanges (see [5,6,23]), while the plasmon mass is a property of time-like gluons [25]. Therefore, we only need to know the two screening masses μ_E and μ_M, in order to generalize the effective cross section to non-zero magnetic mass.

2.2. Modification of $f(\boldsymbol{k},\boldsymbol{q},x)$ due to magnetic screening

As we discussed above, the introduction of the magnetic mass leads to the modification of the exchanged and radiated gluon self energy. In this subsection, we study how the introduction of the magnetic mass in the radiated gluon self energy modifies the radiative energy loss.

To proceed with this study, we note that all radiative energy loss calculations [5,9–16] are performed by assuming validity of the soft gluon ($\omega \ll E$) and soft rescattering ($\omega \gg |\boldsymbol{k}| \sim |\boldsymbol{q}| \sim q_0, q_z$) approximations. Within these approximations, we showed that in the finite temperature QCD medium radiated gluons have similar dispersion relation as in the vacuum, with the difference that the gluons now acquire a "mass" [24]. We also showed that the gluon mass in the medium is approximately equal to the value of gluon self energy at $x = 1$ [24,30] (so-called asymptotic mass $m_\infty = \sqrt{\Pi_T(x=1)}$).

Therefore, analogously to the previous section, we see that the dependence of the $f(\boldsymbol{k},\boldsymbol{q},x)$ on gluon self energy reduces to just a single number: $\Pi_T(x=1)$, which is defined as a square of gluon mass m_g. Due to this, instead of knowing the full gluon propagator, we only need to know how m_g changes in order to obtain how $f(\boldsymbol{k},\boldsymbol{q},x)$ is modified in the case of non-zero magnetic mass.

In principle, gluon mass may change with the introduction of non-zero magnetic screening, but (to our knowledge) no study up to now addressed how non-perturbative calculations would modify the gluon asymptotic mass. Consequently, our approach in the next section is to introduce an ansatz in order to numerically investigate how perturbations of m_g, for a magnitude corresponding to magnetic mass, change radiative energy loss results.

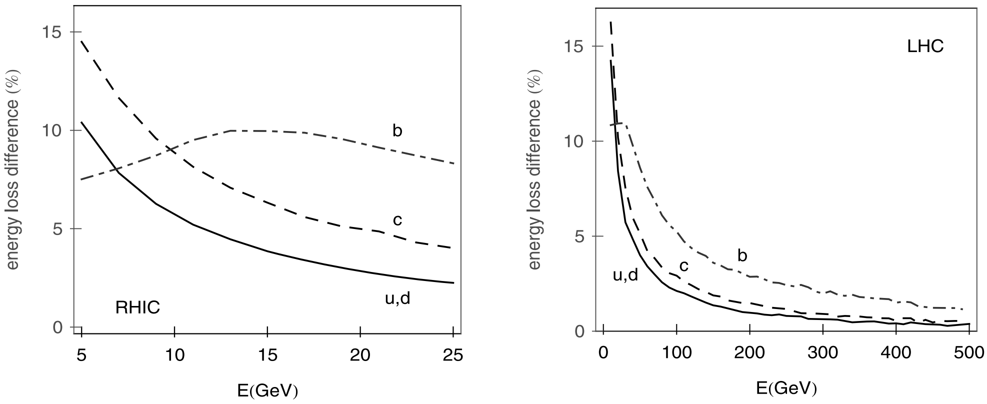

Fig. 1. The percentage difference between energy losses for gluon mass $M_g = \mu_E/\sqrt{2}$ and $M_g = \sqrt{\frac{\mu_E^2+\mu_M^2}{2}}$ is shown as a function of initial jet energy. Full, dashed and dot-dashed curves correspond to light, charm and bottom quark respectively. For left (right) panel, we assume a medium of temperature $T = 225$ ($T = 400$) MeV, which corresponds to RHIC (LHC) conditions.

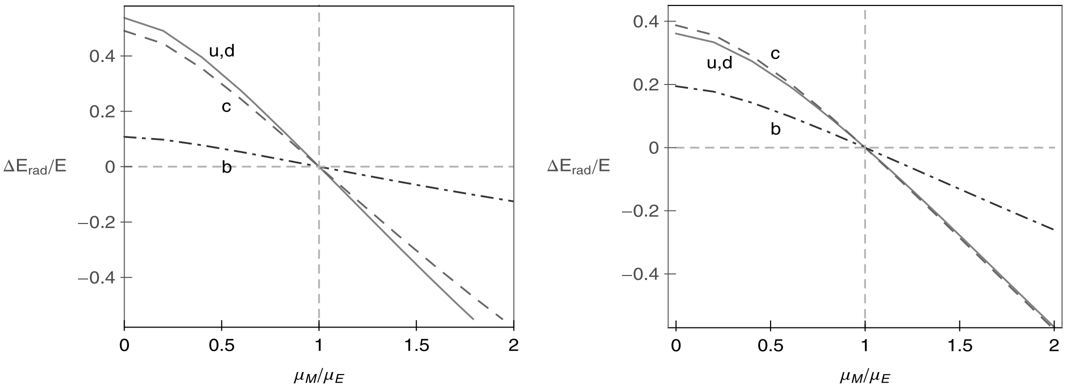

Fig. 2. Fractional radiative energy loss is shown as a function of magnetic to electric mass ratio. Assumed path length is $L = 5$ fm and initial jet energy is 10 (25) GeV for a left (right) panel. Full, dashed and dot-dashed curves correspond to light, charm and bottom quark respectively. Note that for both panels, we assume a medium of temperature $T = 225$ MeV ("RHIC conditions").

2.3. Modification of the energy loss expression due to magnetic screening

After replacing the effective cross section $v(\boldsymbol{q})$ (see Eq. (2.9)) into Eq. (2.1), the total energy loss becomes

$$\frac{\Delta E_{\rm rad}}{E} = \frac{C_R \alpha_s}{\pi} \frac{L}{\lambda_{\rm dyn}} \left(\mu_E^2 - \mu_M^2\right) \int dx \frac{d^2k}{\pi} \frac{d^2q}{\pi} \times \frac{1}{(\boldsymbol{q}^2+\mu_M^2)(\boldsymbol{q}^2+\mu_E^2)} f(\boldsymbol{k}, \boldsymbol{q}, x), \tag{2.10}$$

where $f(\boldsymbol{k}, \boldsymbol{q}, x)$ is given by Eq. (2.2). Note that in Eq. (2.2), $\chi \equiv M^2x^2 + M_g^2$, where the gluon mass M_g can now be different from $m_g = \mu_E/\sqrt{2}$ (see the previous subsection).

2.4. A constraint on the magnetic mass range

We first discuss an interesting observation, that follows directly from Eq. (2.10): Since the integrand in Eq. (2.10) is positive definite, if magnetic mass becomes larger than electric mass, the net energy loss becomes negative. Therefore, if magnetic mass is larger than electric mass, the quark jet would, overall, start to gain (instead of lose) energy in this type of plasma. The origin for this effect can be traced from Eq. (2.8): if the magnetic mass is larger than electric mass, the energy gain from magnetic contribution becomes so large, that it, overall, leads to the total energy gain of the jet. One should note that such a gain would involve transfer of energy of disordered motion of plasma constituents, to energy of ordered jet motion. Such transfer of "low" to "high" quality energy would be in a violation of the second law of thermodynamics. From this may follow that it is impossible to create a plasma with magnetic mass larger than electric, which places a fundamental limit on magnetic mass range. Indeed, in an agreement with this limit, various non-perturbative approaches [18–21] suggest that, at RHIC and LHC, $0.4 < \mu_M/\mu_E < 0.6$. The other possibility is that pQCD cannot be applied for cases where magnetic mass is larger than electric, since calculations in this regime lead to apparent physical inconsistencies.

3. Numerical results

In this section, we numerically study how the inclusion of non-zero magnetic mass modifies the energy loss results. To address this, we consider a quark–gluon plasma of temperature $T = 225$ MeV, with $n_f = 2.5$ effective light quark flavors and strong interaction strength $\alpha_s = 0.3$, as representative of average conditions encountered in Au + Au collisions at RHIC. For the light quark jets we assume that their mass is dominated by the thermal mass $M = \mu/\sqrt{6}$, where $\mu = gT\sqrt{1+N_f/6} \approx 0.5$ GeV is the Debye screening mass. The charm mass is taken to be $M = 1.2$ GeV, and for the bottom mass we use $M = 4.75$ GeV. To simulate (average) conditions in Pb + Pb collisions at the LHC, we use the temperature of the medium of $T = 400$ MeV.

We first investigate how possible changes of gluon mass due to non-zero magnetic screening may change radiative energy loss (see the previous section). To investigate this, we introduce an ansatz

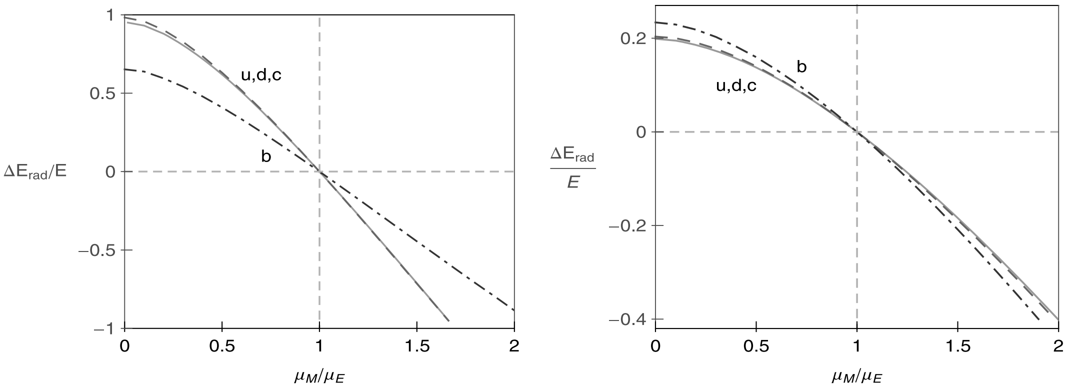

Fig. 3. Fractional radiative energy loss is shown as a function of magnetic to electric mass ratio. Assumed path length is $L = 5$ fm and initial jet energy is 50 (500) GeV for a left (right) panel. Full, dashed and dot-dashed curves correspond to light, charm and bottom quark respectively. Note that for both panels, we assume a medium of temperature $T = 400$ MeV ("LHC conditions").

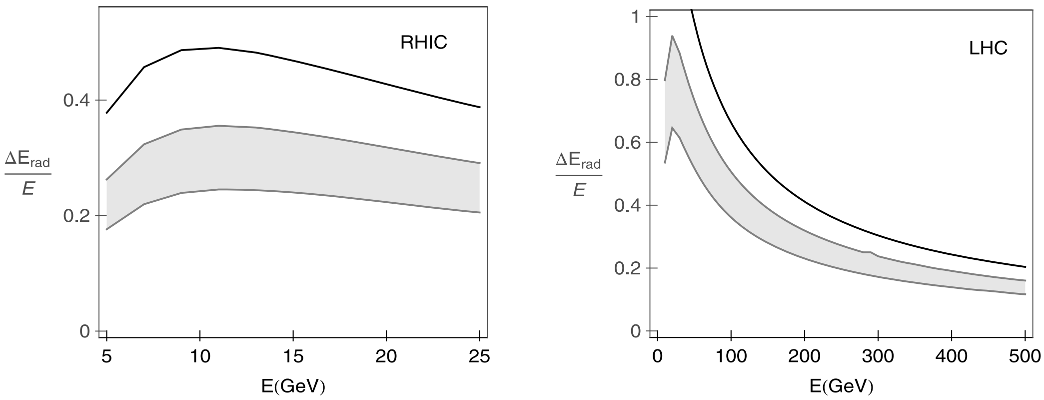

Fig. 4. Fractional radiative energy loss for an assumed path length $L = 5$ fm as a function of momentum for charm quarks. Left (right) panel corresponds to RHIC (LHC) conditions. Full curve corresponds to the case when magnetic mass is zero. Gray band corresponds to the energy loss when magnetic mass is non-zero (i.e. $0.4 < \mu_M/\mu_E < 0.6$). Upper (lower) boundary of the band corresponds to the case $\mu_M/\mu_E = 0.4$ ($\mu_M/\mu_E = 0.6$).

that both electric and magnetic masses equally contribute to gluon self energy at $x = 1$ (i.e. $M_g = \sqrt{\frac{\mu_E^2+\mu_M^2}{2}}$). With this ansatz, which changes the gluon mass for a magnitude comparable to magnetic mass, we obtain a small (less than 10%) change in radiative energy loss for RHIC and negligible change for LHC case (see Fig. 1)). (The only exception is when the initial jet energy $E \lesssim 10$GeV, where soft gluon-soft rescattering approximation becomes less valid.) For simplicity, we will therefore further assume that the gluon mass of radiated gluon remains the same as in [5,24], i.e. that $M_g = \mu_E/\sqrt{2}$. Consequently, in the rest of this section, we numerically study how the inclusion of magnetic mass into the effective cross section modifies the energy loss results compared to the results presented in [5].

Energy loss dependence on the magnetic mass is shown in Figs. 2 and 3 for, respectively, RHIC and LHC case. For both experiments, the results are shown for two characteristic energies, lower and higher. As expected, we see that at RHIC conditions, charm and light quarks show similar energy loss dependence, while energy loss dependence for bottom quark is significantly lower. On the other hand, for LHC conditions, we see that, as the jet energy increases, the energy loss dependences for all quarks approach each other. We also see that the energy loss decreases with the increase in magnetic mass. Importantly, when magnetic masses becomes larger than electric mass, the net energy loss becomes negative, as discussed in the previous section. In Fig. 4, we show momentum dependence of fractional energy loss, where we concentrate on the range $0.4 < \mu_M/\mu_E < 0.6$ (the gray band), as suggested by various non-perturbative approaches [18–21]; we see that finite magnetic mass reduces the energy loss in dynamical QCD medium by 25%–50%.

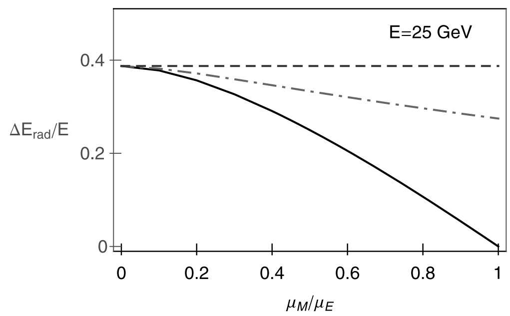

Fig. 5. Fractional radiative energy loss for charm quark as a function of magnetic to electric mass ratio is shown by full curve. Dot-dashed curve shows what would be the energy loss if the magnetic mass correction is only in the denominator. Dashed curve shows the energy loss when $\mu_M = 0$ and is presented here for comparison. Assumed path length is $L = 5$ fm and initial jet energy is 25 GeV. Note that for both panels, we assume a medium of temperature $T = 225$ MeV ("RHIC conditions").

It is interesting to note that, contrary to what one may naively expect, majority of the energy loss decrease does not come from the introduction of magnetic screening in the denominator of the effective cross section. To demonstrate this, in Fig. 5 dot-dashed line shows what would be the energy loss if the magnetic mass was only "by-hand" introduced in the denominator of the effective cross section, while dashed curve shows the result when magnetic mass is introduced both in the numerator and denominator (see

Eq. (2.10)). From the figure, we see that majority of the decrease in the energy loss actually comes from the presence of the magnetic mass in the numerator of the energy loss expression. For example, for the ratio $\mu_M/\mu_E = 0.5$, 25% decrease in the energy loss comes from the presence of the magnetic mass in the numerator, while only 14% decrease comes from the presence of magnetic screening in the denominator of the effective cross section. The reason behind this is that introduction of magnetic screening in the denominator of effective cross section does not regulate the logarithmic divergence in Eq. (2.10). That is, the divergence is already naturally regulated in Eq. (2.1) by taking all the relevant diagrams into account [5,6]. On the other hand, presence of the magnetic mass in the numerator leads to a subtraction of the squares of electric and magnetic masses. Since, according to the non-perturbative approaches [18–21], the two masses are comparable to each other, this will lead to a notable reduction of the energy loss relative to perturbative HTL ($\mu_M = 0$) result.

Finally, we point that several studies [18,20,21,31] suggest that the electric mass is considerably larger than the leading order pQCD result used in this study. While larger electric mass value would change the overall energy loss results, we note that it would not change the qualitative results presented in this Letter. This is because the electric to magnetic mass ratio is calculated to be between 0.4 and 0.6 [18–21], so that larger electric mass also implies proportionally larger magnetic mass (i.e. the relative importance of magnetic mass remains the same).

4. Summary

This Letter generalizes dynamical energy loss formalism to non-zero magnetic screening. While introduction of magnetic mass into any perturbative calculation is inherently phenomenological, the presented inclusion of the effects of modified gluon self energy into the radiative energy loss formalism is valid as long as a well defined quasiparticle system is assumed. Analysis of the finite magnetic mass effects suggests a constraint that it is impossible to create a plasma with magnetic mass larger than electric. Results presented in this Letter allow including non-zero magnetic screening into jet suppression calculations (for example, see our recent application [32] to jet suppression at 200 GeV Au + Au collisions at RHIC), and open a possibility for more accurate mapping of QGP properties.

Acknowledgements

Valuable discussions with Joseph Kapusta, Antony Rebhan, and Miklos Gyulassy are gratefully acknowledged. This work is supported by Marie Curie International Reintegration Grant within the 7th European Community Framework Programme (PIRG08-GA-2010-276913) and by the Ministry of Science and Technological Development of the Republic of Serbia, under projects No. ON171004 and ON173052. Marko Djordjevic is supported in part by Marie Curie International Reintegration Grant within the 7th European Community Framework Programme (PIRG08-GA-2010-276996).

References

[1] D. d'Enterria, B. Betz, Lect. Notes Phys. 785 (2010) 285.
[2] M. Gyulassy, Lect. Notes Phys. 583 (2002) 37.
[3] N. Brambilla, et al., hep-ph/0412158, 2004.
[4] M. Guylassy, I. Vitev, X.N. Wang, B.W. Zhang, in: R.C. Hwa, X.N. Wang (Eds.), Quark Gluon Plasma, vol. 3, Singapore, World Scientific, 2003, p. 123.
[5] M. Djordjevic, Phys. Rev. C 80 (2009) 064909.
[6] M. Djordjevic, U. Heinz, Phys. Rev. Lett. 101 (2008) 022302.
[7] S. Caron-Huot, Phys. Rev. D 79 (2009) 065039.
[8] S. Wicks, arXiv:0804.4704 [nucl-th].
[9] M. Gyulassy, P. Levai, I. Vitev, Nucl. Phys. B 594 (2001) 371.
[10] M. Gyulassy, X.N. Wang, Nucl. Phys. B 420 (1994) 583; X.N. Wang, M. Gyulassy, M. Plumer, Phys. Rev. D 51 (1995) 3436.
[11] U.A. Wiedemann, Nucl. Phys. B 588 (2000) 303; U.A. Wiedemann, Nucl. Phys. B 582 (2000) 409.
[12] E. Wang, X.N. Wang, Phys. Rev. Lett. 87 (2001) 142301; X.N. Wang, X.F. Guo, Nucl. Phys. A 696 (2001) 788; X.F. Guo, X.N. Wang, Phys. Rev. Lett. 85 (2000) 3591.
[13] N. Armesto, C.A. Salgado, U.A. Wiedemann, Phys. Rev. D 69 (2004) 114003.
[14] M. Djordjevic, M. Gyulassy, Phys. Lett. B 560 (2003) 37; M. Djordjevic, M. Gyulassy, Nucl. Phys. A 733 (2004) 265.
[15] M. Djordjevic, Phys. Rev. C 73 (2006) 044912.
[16] P. Arnold, G.D. Moore, L.G. Yaffe, JHEP 0111 (2001) 057; P. Arnold, G.D. Moore, L.G. Yaffe, JHEP 0206 (2002) 030; P. Arnold, G.D. Moore, L.G. Yaffe, JHEP 0301 (2003) 030.
[17] M. Gyulassy, Physics 2 (2009) 107.
[18] Yu. Maezawa, et al., WHOT-QCD Collaboration, Phys. Rev. D 81 (2010) 091501; Yu. Maezawa, et al., WHOT-QCD Collaboration, PoS Lattice (2008) 194.
[19] A. Nakamura, T. Saito, S. Sakai, Phys. Rev. D 69 (2004) 014506.
[20] A. Hart, M. Laine, O. Philipsen, Nucl. Phys. B 586 (2000) 443.
[21] D. Bak, A. Karch, L.G. Yaffe, JHEP 0708 (2007) 049.
[22] Note that, the mean free path of particles in dynamical QCD medium is zero, since the integral of effective cross section in dynamical QCD medium is divergent. λ_{dyn} is named "dynamical mean free path" in [23], in order to make a formal analogy to the energy loss in static QCD medium and enable a direct comparison between energy losses in dynamical and static QCD medium.
[23] M. Djordjevic, U. Heinz, Phys. Rev. C 77 (2008) 024905.
[24] M. Djordjevic, M. Gyulassy, Phys. Rev. C 68 (2003) 034914.
[25] P. Aurenche, F. Gelis, H. Zaraket, JHEP 0205 (2002) 043.
[26] M. Djordjevic, arXiv:1105.4288 [nucl-th].
[27] R.L. Kobes, G. Kunstatter, A. Rebhan, Phys. Rev. Lett. 64 (1990) 2992.
[28] E. Braaten, R.D. Pisarski, Phys. Rev. D 42 (1990) 2156.
[29] M. Dirks, A. Niegawa, K. Okano, Phys. Lett. B 461 (1999) 131.
[30] A. Rebhan, Lect. Notes Phys. 583 (2002) 161.
[31] S. Caron-Huot, Phys. Rev. D 79 (2009) 125002.
[32] M. Djordjevic, arXiv:1105.6082 [nucl-th].